Freestream Velocity Corrections for Two-Dimensional Testing with Splitter Plates

Philippe Giguère* and Michael S. Selig†

University of Illinois at Urbana–Champaign, Urbana, Illinois 61801

The velocity correction method for two-dimensional wind-tunnel testing is expanded for the case of testing airfoils between splitter plates. Despite the common use of splitter plates, the peculiar effects of this testing arrangement on the velocity correction are not well documented. The use of splitter plates in the test section has several advantages, but there are unfortunate consequences (such as spillage, entrainment, and blockage to varying degrees) that require the freestream velocity to be measured directly between the splitter plates with the airfoil in the test section. In this case, the standard velocity correction for wall interference is not sufficient. An additional correction must be made to account for the change in velocity ahead of the airfoil model caused by the circulation about the airfoil. The results reveal that failing to correct for the circulation effect can yield significant errors in the aerodynamic coefficients. The proposed velocity measurement and correction method provides results that are in agreement with data obtained in the NASA Langley Research Center low-turbulence pressure tunnel facility. The method can be readily implemented in the data acquisition and reduction process.

Nomenclature

b	= vertical distance between the tunnel floor and the airfoil usually, $H/2$
C_d	= airfoil drag coefficient
C_l	= airfoil lift coefficient
c	= airfoil chord
F	= complex potential function
H	= height of the test section
h	= vertical distance between the floor of the wind tunnel and the pitot-static tube
k	= velocity ratio, V_m/V_∞
k_x	= influence coefficient for the x component of the induced velocity at the pitot-static tube
k_y	= influence coefficient for the y component of the induced velocity at the pitot-static tube
L	= horizontal distance between the airfoil leading edge and the static orifices on the pitot-static tube
L_u	= uncorrected lift (measured lift)
l	= horizontal distance between the airfoil quarter chord and the static orifices on the pitot-static tube
Q	= source strength
q	= dynamic pressure, $\frac{1}{2}\rho V^2$
q_p	= dynamic pressure at pitot-static tube
q_∞	= freestream dynamic pressure
Δq	= $q_\infty - q_p$
r	= distance from the leading edge of the airfoil model to its axis of rotation
u	= induced velocity in the x direction at the pitot-static tube
V_m	= velocity at the model
V_p	= velocity measured by the pitot-static tube
V_u	= uncorrected or measured upstream velocity
V_∞	= freestream velocity
v	= induced velocity in the y direction at the pitot-static tube
z	= $x + iy$
z_p	= location of the pitot-static tube in the z plane
α	= angle of attack
β	= induced yaw angle at the pitot-static tube
Γ	= circulation
ϵ_{sb}	= solid blockage correction factor
ϵ_{wb}	= wake blockage correction factor
ζ	= $\xi + i\eta$
ζ_p	= location of the pitot-static tube in the ζ plane
$\zeta_v, \zeta_{\bar{v}}$	= location of the vortices in the ζ plane
ρ	= fluid density

Introduction

THE use of splitter plates (sometimes called endplates) in a test section for two-dimensional wind-tunnel testing is rather common.[1–12] For large wind tunnels, splitter plates in the test section can provide more suitable dimensions for two-dimensional testing within the original test section. In such cases, the splitter plates are often referred to as two-dimensional inserts.[6] In some instances, splitter plates are used to allow for the placement of the measuring apparatus totally or in part of the test section, while ensuring an unperturbed flow about the model in the center channel between the splitter plates.[1,2] Another advantage is that splitter plates provide thinner boundary layers than the ones along the wind tunnel walls. The reduction in test section size, the placement of the measuring apparatus in the test section, and the generation of fresh boundary layers are all beneficial effects that make the use of splitter plates advantageous for airfoil testing.

There are, however, some unfortunate consequences related to the insertion of splitter plates in a test section. Specifically, there are three main effects to be considered. First, owing to the presence of the airfoil model and its wake, there can be spillage between the splitter plates and the actual wind-tunnel walls.[1–12] This spillage effect (Fig. 1a) is largely a function of the wake size and can be reduced if dummy models are added between the splitter plates and the tunnel walls[13] or compensated if remotely movable trailing-edge flaps are fitted on the splitter plates.[14] (Note that in Fig. 1a, the effect is exaggerated.) The use of dummy models and removable trailing-edge flaps, however, has some drawbacks. As mentioned by van den Berg,[13] the dummy models will stall earlier at large angles of attack, thereby still making the determination of the freestream velocity a difficult task. Relying on movable trailing-edge flaps to cancel spillage requires monitoring of the dynamic pressure not only in the center channel but also between the splitter plates and the tunnel walls, thus complicating the testing apparatus. Second, there can be entrainment of the flow if the splitter plates are positioned too close to the tunnel walls. The entrainment or sidewall-wake blockage effect (Fig. 1b) is caused by the growing boundary layer on the wind-tunnel wall and splitter plate, which converge toward

a) Spillage effect
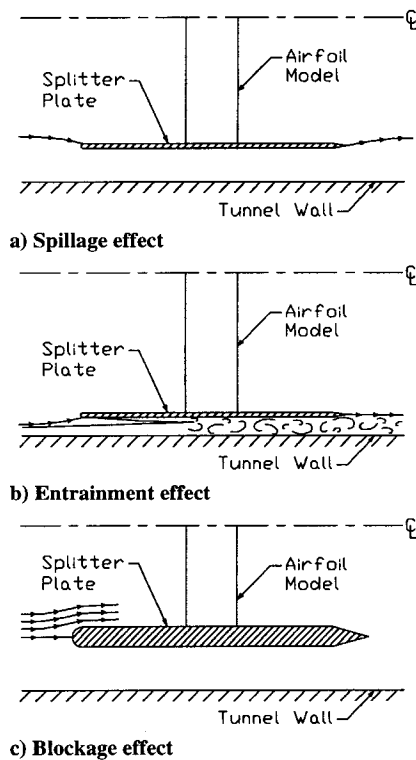

b) Entrainment effect

c) Blockage effect

Fig. 1   Effects of splitter plate in test section.

each other. In effect, the converging boundary layers, which may or may not produce a confluent boundary layer, restrict the flow between the splitter plates and the tunnel walls. Third (Fig. 1c), there can be a blockage effect owing to thick splitter plates that house instrumentation.[7-10]

The amount of entrainment, blockage, and more importantly spillage is difficult if not impossible to ascertain. The main consequence of the aforementioned effects is that the velocity measured ahead of the splitter plates is not equal to that experienced by the model. Consequently, the velocity in the center channel between the splitter plates cannot be calibrated against an upstream flow quantity, but rather the velocity must be measured directly between the splitter plates. Measuring the velocity at that location, however, requires some special considerations because the velocity will be influenced by the circulation about the airfoil: the shorter the length of the splitter plates ahead of the airfoil, the greater the influence of the airfoil circulation on the velocity measurements. Therefore, correcting the velocity measurements for the effect of circulation is of primary importance because the aerodynamic coefficients are normalized by the dynamic pressure.

In most airfoil testing experiments, the wind-tunnel boundary corrections that are used are those taken from Rae and Pope.[14] In this classical reference, however, the specific, yet common, case of using splitter plates in the test section is not fully addressed. Even though the circulation effect has been recognized[7,11] and splitter plates are commonly used for airfoil testing, very little has been documented in the literature and no systematic study of this effect has been conducted. Thus, there is a need to document 1) the additional velocity correction for splitter plates and 2) the implementation of the correction method.

The main objective of the present paper is to provide a velocity correction method that can be easily implemented in the data acquisition and reduction process. Also, the overall magnitude of the velocity correction is assessed over a range of test conditions, velocity measurement locations, and tunnel heights. The results can be used to gauge the magnitude of the circulation effect for particular experimental setups that make use of splitter plates.

Velocity Correction

When splitter plates are used, the velocity correction can be performed in two steps. The velocity at the probe can first be corrected for the circulation effect, and then the velocity at the model can

be computed from the standard velocity correction method for wall interference.[14] By way of introduction, the standard velocity correction is briefly reviewed before presenting the analysis and discussion of the circulation effect. The analysis is based on the use of a pitot-static tube for the measurement of the dynamic pressure between the splitter plates and ahead of the model.

Standard Velocity Correction

The presence of the airfoil model and its wake in a test section causes an increase in velocity as the air flows over the airfoil. The velocity correction is then based on the effect of solid and wake blockage and can be written as[14]

$$V_m = V_u(1 + \epsilon_{sb} + \epsilon_{wb}) \tag{1}$$

The solid blockage correction factor ϵ_{sb} is a function of the airfoil model and test section dimensions, and the wake blockage correction factor ϵ_{wb} is a function of the airfoil chord, tunnel height (for a model mounted horizontally), and drag coefficient.[14]

Another factor that must be considered in the velocity corrections is related to the increase in velocity through the test section caused by the boundary-layer growth along the tunnel walls. To account for boundary-layer growth, either the splitter plates (or tunnel walls) can be appropriately diverged so that the change in the velocity through the test section is negligible. Otherwise, a calibration can be done with the airfoil out of the test section. By measuring both the velocity upstream (but between the splitter plates if used) and the velocity at the model, one can obtain a calibration curve that relates the increase in velocity from the upstream position to the model location as a function of freestream velocity. The freestream velocity at the model V_m is then related to the upstream velocity V_u. This calibration curve can be expressed as

$$V_m = kV_u \tag{2}$$

where k is a function of V_u.

This velocity correction that accounts for the effect of the boundary-layer growth can be combined with the previous velocity correction given by Eq. (1). Therefore, the standard velocity correction is

$$V_m = kV_u(1 + \epsilon_{sb} + \epsilon_{wb}) \tag{3}$$

Circulation Effect

The additional velocity correction proposed here is a freestream velocity correction that accounts for the circulation effect. As discussed earlier, the freestream velocity must be measured between the splitter plates, and as a result the pitot-static tube used to measure dynamic pressure is influenced by the circulation effect. Consequently, at the pitot-static tube, there is an induced velocity that depends on the amount of lift generated by the airfoil model: the greater the lift on the model, and thus the greater the circulation, the greater the induced velocity at the pitot-static tube. This circulation effect is, of course, also a function of the distance between the airfoil and the pitot-static tube. In most practical situations, however, the length of the splitter plates in front of the airfoil is usually small because one of the main advantages of using splitter plates is to minimize the wall boundary-layer thickness at the model/wall juncture.

At this point, it is important to mention that the circulation effect is not only associated with the use of splitter plates. The circulation effect is also important whenever the freestream velocity is being measured in the vicinity of the airfoil model. When there are no splitter plates in the test section, however, a calibration of the freestream velocity in an empty (model out) configuration with the difference in static pressure in the wind-tunnel nozzle is possible. In that case, as will be shown, the circulation effect is usually negligible because the static pressure ports at the entrance of the test section are often relatively far away from the airfoil model.

An assessment of the circulation effect on the freestream velocity requires knowledge of the induced velocity at the pitot-static tube or more generally at the location where the velocity is being measured. To obtain a mathematical expression for the induced velocity, the airfoil is modeled with a single vortex (bound vortex) at the quarter chord. To simulate the presence of the tunnel walls, an infinite image
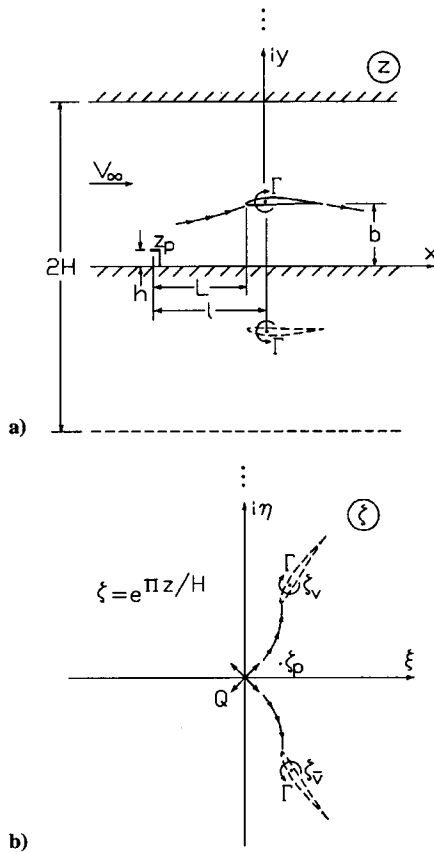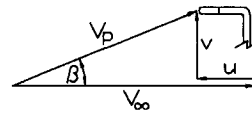
Fig. 3 Velocity diagram at the pitot-static tube (positive lift assumed).

where

$$A = (e^{-\pi l/H} + e^{\pi l/H}) \cos(\pi h/H) - 2\cos(\pi b/H) \quad (9a)$$

$$B = (e^{-\pi l/H} - e^{\pi l/H}) \sin(\pi h/H) \quad (9b)$$

Thus, the x and y components of the induced velocity at the pitot-static tube can be expressed as

$$u = k_x \Gamma/c \quad (10a)$$

$$v = k_y \Gamma/c \quad (10b)$$

where

$$k_x = \frac{-cA\sin(\pi b/H)}{H(A^2 + B^2)} \quad (11a)$$

$$k_y = \frac{-cB\sin(\pi b/H)}{H(A^2 + B^2)} \quad (11b)$$

Note that these coefficients will depend on the angle of attack if the model rotates about any point other than the quarter chord where the bound vortex is modeled.

To compute the induced velocities, an expression for the circulation is required and is given by the Kutta–Joukowski theorem

$$\Gamma = L_u/\rho V_\infty b = \tfrac{1}{2} V_\infty c\, C_{lu} \quad (12)$$

From the velocity diagram at the probe shown in Fig. 3 and noting that u as computed with Eq. (9a) is negative, the freestream velocity can be expressed as

$$V_\infty = V_p \cos\beta - u \quad (13)$$

where

$$\beta = \tan^{-1}\left[\frac{k_y C_{lu}}{2 + k_x C_{lu}}\right] \quad (14)$$

As mentioned, failing to correct for the circulation effect can yield significant errors in the aerodynamic coefficients of the airfoil tested. The errors on the aerodynamic coefficients are related to the errors on the dynamic pressure, which can be written as

$$\Delta q/q_\infty = 1 - (V_p/V_\infty)^2 \quad (15)$$

Using Eqs. (10a), (12), and (13), Eq. (15) yields

$$\frac{\Delta q}{q_\infty} = 1 - \frac{1}{\cos^2\beta}\left[1 + k_x C_{lu} + \left(\frac{k_x C_{lu}}{2}\right)^2\right] \quad (16)$$

The error on the dynamic pressure is, therefore, a function of the experimental setup and the uncorrected lift coefficient (not corrected for wall effects). More precisely, there are three geometric parameters that influence the velocity measurements: the height H of the test section, the height h of the pitot-static tube above the floor of the test section, and the distance l between the airfoil quarter chord and the static orifices on the pitot-static tube.

Figure 4 shows the extent of the circulation effect on the dynamic pressure for a typical test section size with the pitot-static tube located fairly close to the tunnel floor. In all cases considered, the model is centered in the tunnel, that is, $b = H/2$ (see Fig. 2). As expected, the error increases as the lift coefficient is increased (greater Γ) and decreases as the probe is moved upstream (greater L/c). The error on the dynamic pressure presented in Fig. 4 is significant and should not be neglected when the distance from the airfoil to the entrance of the center channel is less than three to four chord lengths depending on the lift range of the tests. This spacing is typical because, as mentioned earlier, one of the main advantages of

Fig. 2 Geometry of the problem for the evaluation of the circulation effect.

system with vortices of alternating signs is used. The geometry of the problem is shown in Fig. 2a. To obtain an expression for the induced velocity field at the pitot-static tube, the contribution of the bound vortex and each of the images must be added. Instead of summing over the infinite number of images,[15] an exact form for the infinite sum can be found from conformal mapping, as indicated in Fig. 2b.

To obtain the induced velocity at the pitot-static tube at point ζ_p in Fig. 2b, the contribution of the bound vortex and each of the images must be added. Instead of summing over the infinite number of images,[15] conformal mapping via the transformation $\zeta = e^{\pi z/H}$ is used to take the flow in the physical z plane to the ζ plane shown in Fig. 2b. In the ζ plane, the complex potential is given by

$$F = (i\Gamma/2\pi)\,\ell n(\zeta - \zeta_v) - (i\Gamma/2\pi)\,\ell n(\zeta - \zeta_{\bar v}) + (Q/2\pi)\,\ell n\,\zeta \quad (4)$$

The third term is the source contribution ($Q = 2HV_\infty$) that represents the flow far upstream, whereas the remaining two are vortices that represent the bound vortex and its images. The complex velocity in the ζ plane is, therefore,

$$\frac{dF}{d\zeta} = \frac{i\Gamma}{2\pi}\frac{\zeta - \zeta_{\bar v}}{(\zeta - \zeta_v)(\zeta - \zeta_{\bar v})} + \frac{HV_\infty}{\pi\zeta} \quad (5)$$

where

$$\zeta_v = e^{i\pi b/H} \quad (6a)$$

$$\zeta_{\bar v} = e^{-i\pi b/H} \quad (6b)$$

The complex velocity in the z plane at the probe location $z = -l + ih$ is obtained from

$$\frac{dF}{dz} = \frac{dF}{d\zeta}\frac{d\zeta}{dz} = \frac{\pi}{H}\frac{dF}{d\zeta}\zeta \quad (7)$$

which yields

$$\frac{dF}{dz} = -\frac{\Gamma}{H}\frac{A - iB}{A^2 + B^2}\sin\left(\frac{\pi b}{H}\right) + V_\infty \quad (8)$$
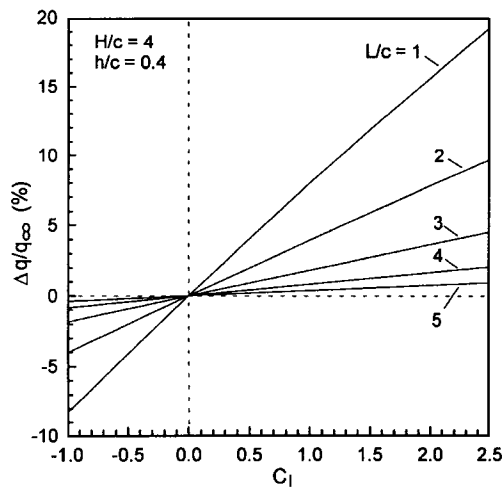
Fig. 4 Error in the dynamic pressure as a function of the lift coefficient; $H/c = 4$ and $h/c = 0.4$.
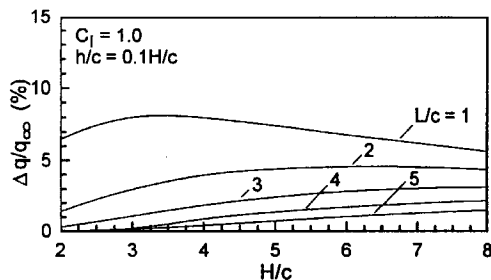
Fig. 5 Error in the dynamic pressure as a function of H/c; $C_l = 1$ and $h/c = 0.1H/c$.

Fig. 6 Error in the dynamic pressure as a function of h/c; $C_l = 1$ and $H/c = 4$.

Fig. 7 Induced yaw angle at the pitot-static tube as a function of H/c; $C_l = 2.5$, $L/c = 1$, and pitot-static tube located at the tunnel centerline.

Fig. 8 Induced yaw angle at the pitot-static tube as a function of h/c; $C_l = 2.5$ and $H/c = 4$.

using splitter plates is to minimize the wall boundary-layer thickness at the model/wall juncture.

The error in the dynamic pressure for different test section heights is presented in Fig. 5. As the height of the test section increases, the overall size of the tunnel also increases, as does the boundary-layer thickness in the test section. It is reasonable to assume that the boundary-layer thickness scales proportionally with the test section height. Thus, for the data shown in Fig. 5, the height of the pitot-static tube above the tunnel floor is kept constant at 10% of the test section height.

The results shown in Fig. 5 indicate the following trends. Again, the error on the dynamic pressure decreases as L/c increases, but the decrease in error is strongly dependent on H/c. Even though the trend for the error in the dynamic pressure with increasing H/c seems to depend on L/c, there is a consistent trend for all L/c ratios considered. As H/c increases, the error in the dynamic pressure first increases until a maximum is reached and then decreases. In Fig. 5, the error in the dynamic pressure only increases with increasing H/c for L/c of 3 or greater but if larger values of H/c had been considered, then the error would have also reached a maximum and then decreased. Actually, the error in the dynamic pressure goes to zero as H/c, and thus h/c, go to infinity. This trend can be traced to two competing effects, which are the orientation of the induced velocity vector from the bound vortex and the images and the vertical distance from the pitot-static tube to each vortex. The more the induced velocity vector is oriented in the horizontal plane (along the x axis), the more it will influence the magnitude of the error in the dynamic pressure. Because the error in the dynamic pressure is mainly a function of the x component of the induced velocity, a smaller induced velocity in magnitude can be compensated by a vector that is more oriented into the x axis.

Until now, the position of the pitot-static tube has been held at 10% of the test section height. The effect of moving the pitot-static tube from the floor of the test section to the centerline of the tunnel is shown in Fig. 6 for the same test section height as that used in Fig. 4. Clearly, the error on the dynamic pressure decreases as h/c increases. Such a trend is not surprising because there can be no horizontal component of the induced velocity at the tunnel centerline.
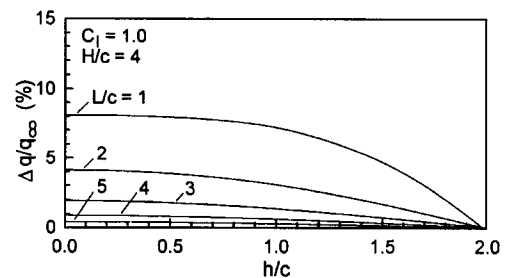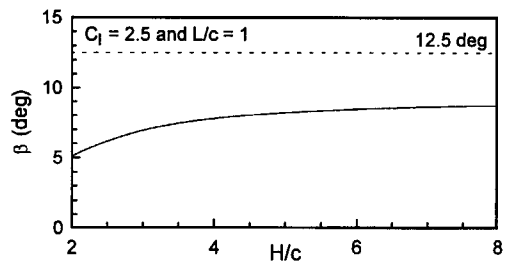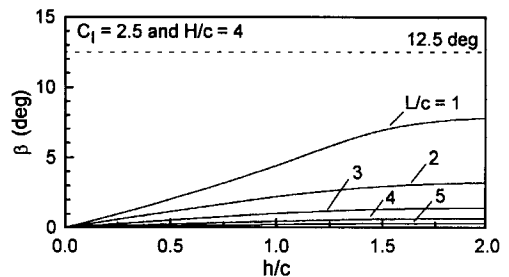
From Figs. 4–6, one could conclude that to minimize the error on the dynamic pressure, the pitot-static tube should be positioned as far forward from the model as possible and at the tunnel centerline. There is, however, another factor to consider, namely, the induced yaw angle at the pitot-static tube. It is important that the yaw angle at the pitot-static tube remain relatively small for accurate dynamic pressure measurements. A standard pitot-static tube is accurate to 0.5% in dynamic pressure for yaw angles less than 12.5 deg (Ref. 14). Figure 7 indicates that even for a lift coefficient as high as 2.5 with the pitot-static tube at the test section centerline and close to the model ($L/c = 1$), the induced yaw angle remains less than 12.5 deg. As indicated in Fig. 8, moving the probe closer to the floor significantly reduces the yaw angle for the same lift coefficient of 2.5. From these results, it is recommended that the pitot-static tube be placed somewhere halfway between the tunnel floor and centerline in order to both minimize the error on the dynamic pressure and avoid flow angularity problems. It is necessary, however, to ensure that the pitot-static tube does not interfere with the flowfield about the model. Thus, the location of the pitot-static tube should be biased toward the tunnel floor.

To account for the circulation effect during actual tests, an iterative procedure must be used because the circulation on the airfoil, which is needed to compute the induced velocities at the pitot-static tube, is a function of the freestream velocity and model lift. Figure 9 outlines the steps involved in this iterative procedure. The proposed velocity correction for the circulation effect must be performed before the standard velocity correction is applied. Therefore, when using splitter plates in the test section, it is necessary to correct the velocity in two steps. The measured velocity is first corrected for the circulation effect. Then, the standard velocity correction is applied to yield the true velocity, Reynolds number, and dynamic pressure at the model.
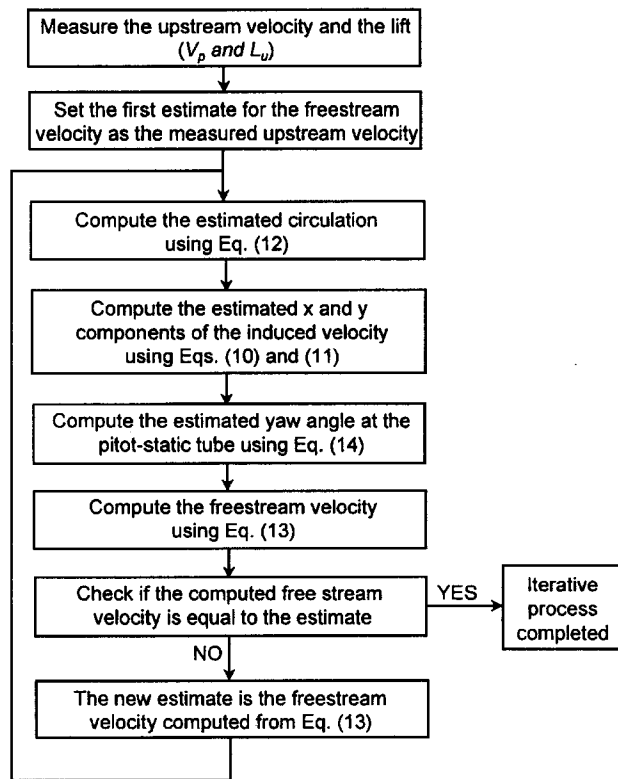
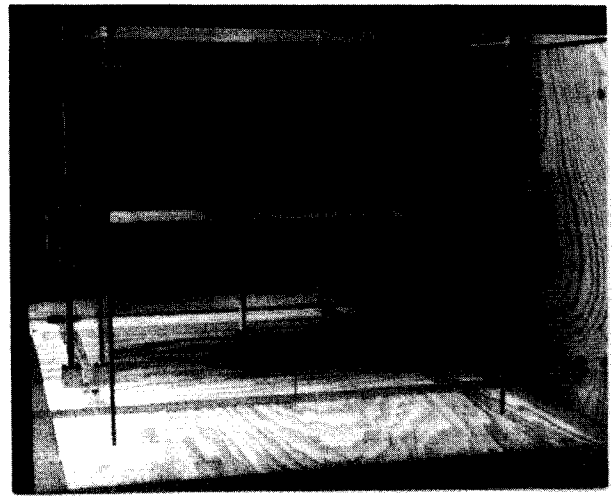Fig. 9   Flowchart to solve for the freestream velocity.

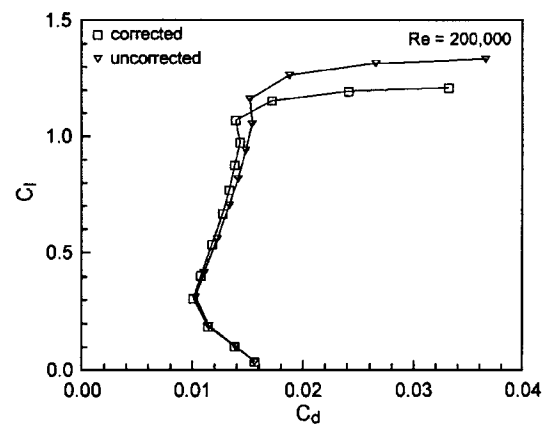Fig. 10   Photograph of the testing arrangement with splitter plates.

Fig. 11   E387 airfoil drag polar with and without applying the additional velocity correction for circulation effect for $Re = 2 \times 10^5$.

The accuracy of the correction method depends on the accuracy of the analytical model. As described, a single vortex is used to represent the airfoil and an infinite image system replaces the tunnel walls. The method could be further refined by distributing the vorticity along the chord or, if more accuracy is desired, along a mean camber line. These refinements could be especially useful for aft-loaded airfoils, which have the center of vorticity aft of the quarter-chord point.

Although the error in dynamic pressure is discussed in terms of the four variables C_l, h/c, H/c, and L/c, a simpler form exists involving only $\Gamma/V_\infty H$, L/H, and h/H, where the chord c has been removed. The former approach is favored for the purposes of discussion as presented.

Validation

To validate the correction method, it was applied to the low Reynolds number test setup used at the University of Illinois at Urbana–Champaign (UIUC) Subsonic Aerodynamics Laboratory. After a brief description of the wind tunnel and the measurement techniques, results that further illustrate the importance of correcting for the circulation effect are presented and discussed. More detailed information regarding the wind tunnel and the measurement techniques can be found in Refs. 2 and 3.

Wind Tunnel and Model Description

The UIUC low-turbulence subsonic wind tunnel is an open-return wind tunnel with a test section 0.857 m (2.813 ft) high by 1.219 m (4 ft) wide. The 0.305-m (1-ft) chord airfoil models were mounted horizontally between two 1.829-m- (6-ft-) long Plexiglas® splitter plates to isolate the ends of the model from the wind-tunnel side-wall boundary layers and the support hardware (as shown in Fig. 10). With the splitter plates, the width of the test section was reduced to 0.854 m (2.802 ft). The average accuracy of the wind-tunnel model was 0.12 mm (0.0046 in.).[16]

Measurement Techniques

The lift was measured using a strain gauge load cell (Interface SM-25) having an accuracy of ±0.01% of the rated output. Drag was determined from the momentum deficit method with two pitot tubes mounted on a traversing mechanism 1.25 chord lengths behind the trailing edge of the model. For each angle of attack, drag measurements were taken at four spanwise locations spaced 76.2 mm (3 in.) apart. These four drag measurements were then averaged. The upstream dynamic pressure was measured with a standard pitot-static tube (as seen in Fig. 10). The horizontal distance from the leading edge of the airfoil to the static orifices on the pitot-static tube was 0.327 m (1.070 ft), and vertical distance from the floor to the static orifices was 0.133 m (0.435 ft). Each pitot-static tube was connected to an MKS pressure transducer with a full-scale range of 1-mm (0.039-in.) Hg and an accuracy of 0.15% of the full-scale reading. The overall uncertainty is estimated to be 1.5% for both the lift and drag.[16] Finally, the entire data acquisition process was completely automated.

Experimental Results

Lift and drag measurements for the Eppler 387 airfoil were obtained at Reynolds numbers of 2×10^5 and 4.6×10^5. Figure 11 clearly shows the direct effect of neglecting the velocity correction for the circulation effect. The difference in the lift and drag is as high as 8–10% at the higher end of the lift range ($C_l \approx 1$).

As an indication of the validity of the proposed method to account for the circulation effect, the corrected data are compared in Fig. 12 with results from the NASA Langley Research Center low-turbulence pressure tunnel (LTPT).[17] The overall agreement of the results is remarkably good. Furthermore, oil-flow visualization on the E387 airfoil provided upper surface separation and reattachment locations that matched within 1% those found at NASA Langley Research Center LTPT.[18] (Note that no splitter plates were used for the tests performed at NASA Langley Research Center LTPT.) Therefore, the proposed velocity correction method for circulation effect has been successfully validated.
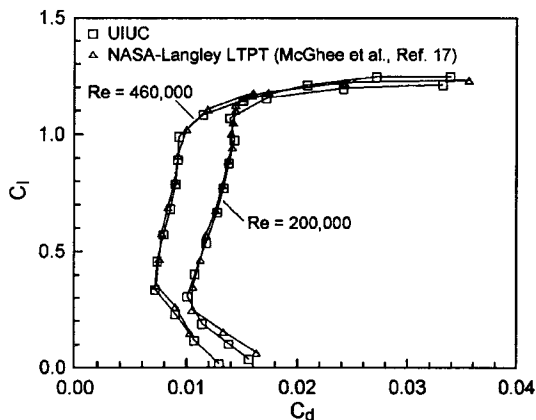
Fig. 12 Comparison of the drag data of the E387 airfoil for $Re = 2 \times 10^5$ and $Re = 4.6 \times 10^5$.

Conclusions

The present study of the effects of splitter plates on the velocity measurement and correction procedure for two-dimensional wind-tunnel experiments have led to the following conclusions.

1) The standard velocity correction for solid and wake blockage, as well as boundary-layer growth, is not sufficient when testing airfoils between endplates because the circulation generated by the airfoil induces a velocity at the pitot-static tube location. Therefore, an additional velocity correction that accounts for this circulation effect must be considered.

2) The circulation effect is not only present in the case of testing airfoils between splitter plates but whenever the velocity is measured in the upwash or downwash of the airfoil model. Failing to measure the freestream velocity in the test section (between the splitter plates when present) and to correct for the circulation effect yields errors in the aerodynamic coefficients that are proportional to the lift coefficient.

3) The proposed velocity correction for the circulation effect coupled with the standard velocity correction provides results that are in agreement with results obtained in the NASA Langley Research Center LTPT facility and can be readily implemented in the data acquisition and reduction process. The correction factors can be obtained from the results presented here or calculated for the particular experimental setup.

Acknowledgments

References

[1]Selig, M. S., Donovan, J. F., and Fraser, D. B., *Airfoils at Low Speeds*, SoarTech, Virginia Beach, VA, 1989, Chap. 2.

[2]Selig, M. S., Guglielmo, J. J., Broeren, A. P., and Giguère, P., *Summary of Low-Speed Airfoil Data—Volume 1*, SoarTech, Virginia Beach, VA, 1995, Chap. 2.

[3]Guglielmo, J. J., "Spanwise Variations in Profile Drag for Airfoils at Low Reynolds Numbers," M.S. Thesis, Dept. of Aeronautical and Astronautical Engineering, Univ. of Illinois, Urbana, IL, May 1996.

[4]Mueller, T. J., and Jansen, B. J., Jr., "Aerodynamic Measurements at Low Reynolds Numbers," AIAA Paper 82-0598, March 1982.

[5]Mueller, T. J., Pohlen, L. J., Conigliaro, P. E., and Jansen, B. J., Jr., "The Influence of Free-Stream Disturbances on Low Reynolds Number Airfoil Experiments," *Experiments in Fluids*, Vol. 1, No. 1, 1983, pp. 3–14.

[6]Nagamatsu, H. T., and Cuche, D. E., "Low Reynolds Number Aerodynamic Characteristics of Low Drag NACA 63-208 Airfoil," *Journal of Aircraft*, Vol. 18, No. 10, 1981, pp. 833–837.

[7]Wentz, W. H., Jr., and Fiscko, K. A., "Wind Tunnel Force and Pressure Tests of a 21% Thick General Aviation Airfoil with 20% Aileron, 25% Slotted Flap and 10% Slot-Lip Spoiler," Wichita State Univ., Rept. AR 77-6, Wichita, KS, Nov. 1977.

[8]Rodgers, E. J., Wentz, W. H., Jr., and Seetharam, H. C., "Instrumentation, Techniques and Data Reduction Associated with Airfoil Testing Programs at Wichita State University," *Advanced Technology Airfoil Research*, Vol. I, NASA CP-2045, Pt. 2, 1979, pp. 539–557.

[9]Biber, K., and Zumwalt, G. W., "Hysteresis Effects on Wind Tunnel Measurements of a Two-Element Airfoil," *AIAA Journal*, Vol. 31, No. 2, 1993, pp. 326–330.

[10]Ranzenbach, R., and Barlow, J., "Cambered Airfoil in Ground Effect—An Experimental and Computational Study," Vehicle Aerodynamics: Wind Tunnels, CFD, Aeroacoustics, and Ground Transportation Systems, SAE SP-1145, Society of Automotive Engineers, Warrendale, PA, 1996, pp. 269–276.

[11]Davis, S., and Satyanarayana, B., "Two-Dimensional Transonic Testing with Splitter Plates," NASA TP-1153, 1978.

[12]Davis, S. S., and Malcom, G. N., "A New Two-Dimensional Oscillating Wing Apparatus for Unsteady Aerodynamics Research," *Advanced Technology Airfoil Research*, Vol. 1, NASA CP-2045, Pt. 2, 1979, pp. 671–688.

[13]van den Berg, B., "Some Notes on Two-Dimensional High-Lift Tests in Wind Tunnels," Lecture Series No. 43 on Assessment of Lift Augmentation Devices, AGARD LS-43-71, 1971, pp. 5-1–5-17.

[14]Rae, W. H., Jr., and Pope, A., *Low-Speed Wind Tunnel Testing*, Wiley, New York, 1984, pp. 93–95, 344–362.

[15]Giguère, P., and Selig, M. S., "Freestream Velocity Measurements and Corrections for Two-Dimensional Testing with Splitter Plates," AIAA Paper 96-2388, June 1996.

[16]Selig, M. S., and Guglielmo, J. J., "High-Lift Low Reynolds Number Airfoil Design," *Journal of Aircraft*, Vol. 34, No. 1, 1997, pp. 72–79.

[17]McGhee, R. J., Jones, G. S., and Jouty, R., "Performance Characteristics from Wind-Tunnel Tests of a Low-Reynolds Number Airfoil," AIAA Paper 88-0607, Jan. 1988.

[18]Lyon, C. A., Selig, M. S., and Broeren, A. P., "Boundary-Layer Trips on Airfoils at Low Reynolds Numbers," AIAA Paper 97-0511, Jan. 1997.

R. W. Wlezien
Associate Editor